



Spinal microglia contribute to cancer-induced pain through system x_C^- -mediated glutamate release

Tanya Miladinovic^{a,b}, Gurmit Singh^{a,b,*}

Abstract

Introduction: Microglial cells, the resident macrophages of the central nervous system, are a key contributor to the generation and maintenance of cancer-induced pain (CIP). In healthy organisms, activated microglia promote recovery through the release of trophic and anti-inflammatory factors to clear toxins and pathogens and support neuronal survival. Chronically activated microglia, however, release toxic substances, including excess glutamate, causing cytotoxicity. Accordingly, rising attention is given to microglia for their role in abnormal physiology and in mediating neurotoxicity.

Objectives: To examine the nociceptive relationship between peripherally-released glutamate and microglial xCT.

Methods: A validated murine model of 4T1 carcinoma cell-induced nociception was used to assess the effect of peripheral tumour on spinal microglial activation and xCT expression. Coculture systems were then used to investigate the direct effect of glutamate released by wildtype and xCT knockdown MDA-MB-231 carcinoma cells on microglial activation, functional system x_C^- activity, and protein levels of interferon regulatory factor 8 (IRF8), a transcription factor implicated in microglia-mediated nociception.

Results: Blockade of system x_C^- with sulfasalazine (SSZ) in vivo attenuated nociception in a 4T1 murine model of CIP and attenuates tumour-induced microglial activation in the dorsal horn of the spinal cord. Furthermore, knockdown of xCT in MDA-MB-231 cells mitigated tumour cell-induced microglial activation and functional system x_C^- activity in vitro.

Conclusions: These data collectively demonstrate that the system xCT antiporter is functionally implicated in CIP and may be particularly relevant to pain progression through microglia. Upregulated xCT in chronically activated spinal microglia may be one pathway to central glutamate cytotoxicity. Microglial xCT may therefore be a valuable target for mitigating CIP.

Keywords: Cancer, Pain, Nociception, System x_C^- , xCT, SLC7A11, Microglia

1. Introduction

Cancer-induced pain (CIP) is a debilitating condition that accompanies late-stage cancer for most patients. As the resident macrophages of the central nervous system (CNS), microglia are a key contributor to the generation and maintenance of pain. In healthy organisms, activated microglia promote recovery, clear pathogens, and support neuronal survival.⁵² Chronically activated microglia, however, release harmful substances, including excess glutamate, causing cytotoxicity.⁶¹ Accordingly, rising attention is

given to microglia for their role in abnormal physiology and mediating neurotoxicity. A growing body of evidence indicates that spinal microglial activation is a hallmark of neuroinflammation and is well-documented in chronic pain^{9,20,47,53} (reviewed in Refs. 57 and 58). Peripheral nerve injury has been shown to induce substantial changes in microglia within the spinal cord,^{1,35,56} and several gliamodifying drugs have been shown to alter pain sensitivity.^{43,54,64} Accumulating evidence also suggests that microglial activation plays a definitive roll in CIP.^{17,18,23,27,62,65}

In their activated state, microglia produce soluble factors, including the ubiquitous cell signalling molecule and major excitatory neurotransmitter glutamate.^{4,5,38} Glutamate dysregulation has been linked to various pathologies by its excitotoxic property and is exchanged with cystine through xCT, the active subunit of the system x_C^- antiporter (reviewed in Refs. 11 and 30). System x_C^- activity and xCT expression are constitutively low in the naive CNS⁴⁴; however, one pathway to neurotoxicity involves the release of glutamate by microglia through system x_C^- .^{3,38–40,63} The system x_C^- transporter is upregulated in microglia in the presence of oxidative stress as a compensatory mechanism for neurons' limited capacity to upregulate this antiporter.⁵ Accordingly, inhibitors of cystine uptake have been shown to inhibit the cytotoxic effects of macrophages through the suppression of glutamate release.⁶³ Activation of spinal microglia is associated with elevated cerebral spinal fluid (CSF) glutamate

Sponsorships or competing interests that may be relevant to content are disclosed at the end of this article.

^a Department of Pathology and Molecular Medicine, Michael G. DeGroote Institute for Pain Research and Care, Medicine, McMaster University, Hamilton, ON, Canada, ^b Department of Pathology and Molecular Medicine, McMaster University, Hamilton, ON, Canada

*Corresponding author. Address: Department of Pathology and Molecular Medicine, McMaster University, 1280 Main St West, Hamilton, ON L8N 3Z5, Canada. Tel.: +1 905 525 9140 x28144. E-mail address: singhg@mcmaster.ca (G. Singh).

Copyright © 2019 The Author(s). Published by Wolters Kluwer Health, Inc. on behalf of The International Association for the Study of Pain. This is an open access article distributed under the Creative Commons Attribution-NoDerivatives License 4.0 (CC BY-ND) which allows for redistribution, commercial and non-commercial, as long as it is passed along unchanged and in whole, with credit to the author.

PR9 4 (2019) e738

<http://dx.doi.org/10.1097/PR9.0000000000000738>

concentrations in rats with sciatic nerve injury,¹⁰ and reduction of CSF glutamate levels through inhibition of glutamate transporter 1 (GLT-1) and glutamate aspartate transporter inhibits formalin-induced nociception.^{36,37}

The relationship between microglia and glutamate is multidimensional. Activated microglia secrete glutamate through system x_C^- ,^{5,21} but are also activated by exogenous glutamate (reviewed in Ref. 34). The presence of glutamate receptors (GluRs) on microglia has therefore been presented as a potential link between inflammation and excitotoxic CNS damage.^{41,55} Given that microglia express various metabotropic and ionotropic GluRs, glutamate released by microglia may act in an autocrine fashion by activating neighboring microglial GluRs (reviewed in Ref. 33).

Our laboratory previously demonstrated the involvement of glutamate in a murine model of CIP^{45,60} and has recently developed a human MDA-MB-231 carcinoma cell line that features a stable shRNA-induced knockdown of *SLC7A11*, the gene which encodes xCT.⁵⁹ To explore the role of xCT in the inflammatory immune response to peripheral tumours, our validated murine model of CIP was used to quantify spinal microglial activation and xCT expression in relation to nociceptive behaviours. We then used an isolated in vitro coculture system to confirm that the observed in vivo effects represented a direct relationship between peripherally released glutamate and reactive spinal microglia.

2. Methods

2.1. Cell cultures

HMC3 human microglia cells (American Type Culture Collection; ATCC, Manassas, VA) were maintained in Eagle's minimum essential medium (EMEM; Life Technologies, Carlsbad, CA). Wildtype MDA-MB-231 triple-negative human mammary gland carcinoma cells (ATCC), shRNA-generated C6 xCT knockdown clones (xCT KD), and pLKO1 empty vector control cells⁵⁹ were maintained in high glucose DMEM (Life Technologies). To maintain xCT knockdown, growth media for xCT KD clones (and empty vector controls) were supplemented with puromycin (1 μ g/mL) daily. As per supplier instructions, microglia were supplemented with 10% fetal bovine serum. 4T1 triple-negative murine carcinoma cells (ATCC) were maintained in RPMI (Life Technologies). All carcinoma cells were supplemented with 10% fetal bovine serum and 1% antibiotic/antimycotic, incubated at 37°C and 5% CO₂, and verified to be mycoplasma free before experimental use.

2.2. Animals

Experimentally naive immunocompetent female BALB/c mice (Charles River Laboratories, Quebec) aged 4 to 6 weeks upon arrival were group-housed at 24°C with a 12-hour light/dark cycle and provided ad libitum access to food and water. All procedures were performed according to guidelines established by the Canadian Council on Animal Care under a protocol reviewed and approved by the Animal Research Ethics Board (AREB) of McMaster University.

2.3. Behavioural test of nociception

A validated syngeneic mouse model of CIP³² was used to characterize the effects of intrafemoral tumour on nociceptive behaviours and spinal microglial xCT. The progression of spontaneous nociception before and after tumour cell inoculation

was monitored using the Dynamic Weight Bearing (DWB) system (BioSeb, Vitrolles, France), a test for pain-related discomfort and postural equilibrium, as previously described.³² Briefly, mice (N = 24) were randomly assigned to treatment groups {4T1 tumour (treated with sulfasalazine [SSZ] or vehicle, n = 8/group) or frozen/heat-killed 4T1 cell sham controls, n = 8} and acclimated to testing environment before data collection. Three behavioural tests were performed before experimental day 0 to establish a stable baseline for normal behaviour, and a video camera provided user-independent spatiotemporal references. Postural disequilibrium was defined as a favouring of the tumour-bearing limb and the resultant shift of weight-bearing to other body parts and was considered indirect evidence of nociception; results are expressed for each animal as a percentage of respective baseline scores.

2.4. Tumour allografts

The 4T1 carcinoma cell line was selected as a model for stage IV human breast cancer as it is highly tumorigenic and invasive, with the growth and metastatic spread of these cells in BALB/c mice closely mirroring human MDA-MB-231 breast cancer in its proliferative and metastatic properties.⁴² Mice were inoculated with 4T1 cells or an equal number of frozen/heat-killed 4T1 sham controls injected percutaneously into the right distal femur to establish tumours, as previously described.^{32,60} Briefly, on experimental day 0, mice were anaesthetized by isoflurane inhalation and injected with buprenorphine (0.05 mg/kg, subcutaneous; Schering-Plough, Kenilworth, NJ) to mitigate surgically induced nociceptive discomfort. Animals were inoculated with 4T1 cells (2×10^4 , suspended in 25- μ L sterile phosphate-buffered saline). The contralateral hindlimb served as a negative control specific to each animal. This method of intrafemoral injection was selected to minimize damage to the surrounding tissues and has been successfully applied in mouse^{32,60} and rat¹² models of bone CIP.

2.5. Drug treatments

Mice were systemically treated with SSZ or vehicle from day 7 after cell inoculation through endpoint. Drug treatment was delayed until day 7 to allow sufficient time for the implanted cells to reliably establish a bone tumour without drug interference, more accurately mimicking clinical conditions. SSZ was dissolved in 1 M NH₄OH and administered through intraperitoneally (i.p.)-implanted mini-osmotic pumps (Alzet model 1002; Durect, Cupertino, CA) at a maximum soluble dose of 6.6 mg/kg/d, based on the mean weight of the mice on day 0 (20 g).

2.6. Transcardial perfusion and tissue collection

Mice were euthanized by transcardial perfusion by day 20 after tumour cell inoculation, or when they no longer bore weight on the afflicted limb. Under sodium pentobarbital anesthetic (90 mg/kg, i.p.), animals were perfused with 100 mL cold PBS, immediately followed by 100 mL cold 4% paraformaldehyde (PFA). Spinal cords were immediately dissected, and lumbar vertebrae 4 (L4) sections were isolated and postfixed in fresh 4% PFA for 48 hours, then processed for immunofluorescent analyses.

2.7. Immunofluorescence

The L4 region of each spinal cord was decalcified in 10% EDTA (Sigma-Aldrich, St. Louis, MO) for 14 days, dehydrated, and paraffin-embedded for histological analyses. Spinal cords were

then coronally sectioned at 5 μm , deparaffinized and rehydrated, exposed to antigen retrieval in EDTA (pH 8, 95°C) for 20 minutes, blocked (Dako protein block) for 2 hours, incubated in respective primary and fluorescent secondary antibodies (**Table 1**), counterstained with DAPI, coverslipped, and imaged using EVOS FL Cell Imaging System. Serial sections were stained, with primary antibodies replaced by respective isotype controls to serve as a negative control specific to each animal.

2.8. Cocultures

HMC3 human microglia were cultured with or without wildtype, xCT KD, or empty vector control MDA-MB-231 carcinoma cells as an in vitro model of peripheral tumour-released glutamate on microglial activation. HMC3 and MDA-MB-231 cells were seeded at 5×10^5 cells/well in 6-well plates and 4- μm pore transwell inserts (Corning, Tewksbury, MA), respectively. Cells adhered to inserts or wells in respective media for 2 hours, then MDA-MB-231 transwell inserts were added to HMC3 plates and cocultured for 24 hours, with EMEM+ and DMEM+/+ media-only negative controls.

2.9. In vitro cell treatments

Lipopolysaccharide (LPS; Sigma-Aldrich), the system x_C^- inhibitor SSZ (Sigma-Aldrich), and L-glutamic acid (Sigma-Aldrich) were prepared in accordance with manufacturer's recommendations in PBS, 1 M NH_4OH , and PBS, respectively, and administered at doses of 1 $\mu\text{g}/\text{mL}$ (LPS), 200 μM (SSZ), and 300 mM (L-glutamic acid).

2.10. Coculture cystine uptake

The cellular uptake of radiolabeled ^{14}C -cystine was quantified in HMC3 cells because cystine uptake is mediated by an exchange with glutamate through system x_C^- . HMC3 cells were cocultured with wildtype, xCT KD, or vector control MDA-MB-231 cells to quantitate the direct effect of peripherally released glutamate on microglial functional system x_C^- activity. The cystine uptake protocol was adapted from previous reports³² and adjusted to include coculture conditions. Briefly, microglia and MDA-MB-231 carcinoma cells were seeded in 6-well plates and transwell inserts, respectively. Treated microglia and co-cultures were incubated for 24 hours, at which point drugs were aspirated or co-culture inserts were removed,

microglia were exposed to ^{14}C -cystine (0.015 mCi/mL) for 20 minutes at 37 °C, washed, and cells were lysed (0.1% Triton-X in 0.1 N NaOH) for 30 minutes. Lysates (100 μL) were quantified in 1 mL of Ecoscint-H scintillation fluid. Values were normalized to milligrams of total protein and compared with ^{14}C -cystine uptake in naive HMC3 cells from the same experimental run.

2.11. Immunocytochemistry

Immunocytochemistry was performed to assess the effect of carcinoma cell-secreted glutamate on microglial activation through morphology and xCT expression. HMC3 microglia were seeded at 10^4 cells/well in 8-well chamber slides (Ibidi, Martinsried, Germany) and treated with LPS (1 $\mu\text{g}/\text{mL}$) or supplemented with complete media from xCT KD or vector-only control cells every 8 hours for 24 hours. Media supplements were gently aspirated, HMC3 cells were washed, fixed with 10% neutral-buffered formalin, permeabilized with 0.1% Triton X-100 for 20 minutes, blocked with 1% bovine serum albumin for 1 hour, incubated in Iba1 and xCT primary antibodies for 1 hour each at room temperature, and visualized using respective secondary antibodies (see **Table 1** for antibody details) with DAPI Fluoroshied counterstain (Thermo Fisher, Waltham, MA) using EVOS FL Cell Imaging System.

2.12. Western blotting

HMC3 cells were treated with 1- μg LPS (or PBS) or cocultured, as above, with MDA-MB-231, xCT KD, or empty vector control, cell inserts for 24 hours to determine the effects of peripheral tumour-secreted glutamate on xCT, interferon regulatory factor 8 (IRF8), signal transducer and activator of transcription 3 (STAT3), and extracellular signal-regulated kinase 1/2 (ERK1/2) protein levels, and quantified by Western blot analysis, as previously described.³² Briefly, total protein concentrations were determined to ensure equal protein loading of whole cell lysates on 10% SDS-PAGE gels and subsequent electrophoretic transfer to PVDF membranes (Immobilon-P; Millipore Corporation, Danvers, MA). Expression levels of target proteins were evaluated using respective primary antibodies with calnexin (90 kDa) as a loading control (**Table 1**), with blocking in 5% skim milk in Tris-buffered saline, 0.1% Tween 20 (TBS-T). Membranes were incubated in respective horseradish peroxidase-conjugated secondary antibodies for 2 hours at room temperature and visualized by

Table 1

Antibodies and respective concentrations ([]) used for Western blotting, immunocytochemistry (ICC), and immunofluorescence (IF) assays.

| Assay | Primary antibody | Supplier; catalogue # | [] | Secondary antibody | Notes |
|------------------|------------------|-----------------------------|----------------------------|---------------------------------|--|
| Western blotting | Calnexin | Santa Cruz; SC-11397 | 1:1000 | HRP-conjugated goat anti-rabbit | |
| | xCT | Novus Biologicals; 300-318 | 1:1000 | HRP-conjugated goat anti-rabbit | |
| | IRF8 | Thermo Scientific; PA520088 | 1:1000 | HRP-conjugated goat anti-rabbit | |
| | Phospho-STAT3 | Cell Signalling; 09145S | 1:1000 | HRP-conjugated goat anti-rabbit | |
| | STAT3 | New England Biolabs; 4904P | 1:1000 | HRP-conjugated goat anti-rabbit | |
| | Phospho-ERK1/2 | Upstate; 05-797 | 1:1000 | HRP-conjugated goat anti-rabbit | |
| | ERK1/2 | Cell Signalling; 9122 | 1:1000 | HRP-conjugated goat anti-rabbit | |
| | Iba1 | Wako; 019-19741 | 1:1000 | HRP-conjugated goat anti-rabbit | |
| | ICC | xCT | Novus Biologicals; 300-318 | 1:500 | Goat anti-rabbit AF488 |
| Iba1 | | Wako; 019-19741 | 1:500 | Goat anti-rabbit AF647 | Blocked with 10% rabbit serum for 1 hour |
| IF | xCT | Novus Biologicals; 300-318 | 1:200 | Goat anti-rabbit AF488 | |
| | Iba1 | Wako; 019-19741 | 1:200 | Goat anti-rabbit AF647 | Blocked with 10% rabbit serum for 1 hour |

enhanced chemiluminescence (ECL-plus kit; GE Healthcare, Chicago, IL) on Amersham Hyperfilm (GE Healthcare). Blots were quantified using densitometry with ImageJ software (US National Institutes of Health), normalized to loading controls, and compared with naive HMC3 cells.

2.13. Statistical analyses

All in vitro data are presented as mean \pm SEM from 3 independent experiments. Individual *t* tests were used to assess the effects of functional system x_C^- activity in cocultures, as measured by ^{14}C -cystine uptake, relative to naive, LPS-stimulated, and wildtype-cocultured microglia. For Western Blot analyses, separate *t* tests were conducted to assess the effect of LPS and coculture conditions on microglial protein levels. For STAT3 and ERK1/2, data are expressed as a percentage of phosphorylated (pSTAT3 and pERK1/2) over respective total protein levels. In vivo and ex vivo data encompass $n = 8/\text{group}$. For behavioural analysis of nociception, a 2 (treatment) \times 2 (test day) repeated-measures analysis of variance followed by Bonferroni multiple comparisons was conducted on DWB data. Immunocytochemical and immunofluorescent images were qualitatively considered, with representative images presented. All analyses were performed using GraphPad Prism 7.0a software (GraphPad Software, Inc, La Jolla, CA) with $\alpha = 0.05$.

3. Results

3.1. Blockade of System x_C^- with SSZ attenuates cancer-induced pain

Tumour-bearing mice demonstrated significantly greater nociceptive behaviours relative to sham controls from day 13 until endpoint, consistent with previously published data from this model³² and our immunocompromised model of CIP using wildtype MDA-MB-231 carcinoma cells.⁶⁰ In accordance with data from immunocompromised MDA-MB-231 tumour-bearing mice, treatment with the system x_C^- inhibitor SSZ delayed behavioural decline in 4T1 tumour-bearing mice, indicated by significantly greater weight borne relative to vehicle-treated tumour-bearing mice from day 13 through endpoint (**Fig. 1**).

3.2. Peripheral tumour alters spinal microglial activity

The number of reactive spinal microglia seemed to increase in the L4 dorsal horn ipsilateral to tumour-inoculated limbs relative to sham, with particular density in laminae I-III (**Fig. 2B**). Regional microglia in tumour-bearing mice appeared vivid in colour, indicated by retracted processes and intense immunofluorescence (**Fig. 2B**, inserts v and vi). Several activated microglia in this region also stained positive for xCT in naive and tumour-bearing mice (**Fig. 2A, B**, inserts iii and vi). Treatment with SSZ abolished xCT in spinal sections confirming the ability of SSZ to reach the target spinal microglia in vivo, and regional microglia were characteristically ramified, highly branched in morphology, with weak Iba1 staining (**Fig. 2C**, insert iii).

3.3. MDA-MB-231 carcinoma cell-released glutamate activates microglia in vitro

Immunocytochemical fluorescent costaining of Iba1 and xCT demonstrated that microglia supplemented with MDA-MB-231 cell complete media are activated in a pattern similar to LPS-activated microglia (**Fig. 3**). This activation was attenuated in the

presence xCT KD cell complete media, supporting the notion that peripherally released glutamate contributes to microglial activation. Naive microglia seemed characteristically ramified, while LPS-stimulated microglial processes were retracted, and fluorescent staining of Iba1 appeared vivid, indicative of increased microglial activation.¹⁶ Activated microglia also exhibited intense xCT staining, with a pattern of increased fluorescence observed directly outside nuclei (**Fig. 3**).

3.4. MDA-MB-231 cell-released glutamate increases microglial cystine uptake in vitro

Treatment with LPS significantly increased ^{14}C -cystine uptake by HMC3 human microglia relative to untreated cultures. Direct stimulation with L-glutamic acid, a quantity analogous to that secreted by MDA-MB-231 carcinoma cells over a 24-hour period (data not shown), increased microglial ^{14}C -cystine uptake in a manner comparable with LPS-stimulated microglia. SSZ significantly decreased microglial ^{14}C -cystine uptake relative to naive cells and abolished LPS-induced increases in microglial ^{14}C -cystine uptake (**Fig. 4**).

In cocultures, microglial ^{14}C -cystine uptake was significantly increased in the presence of both wildtype and vector control MDA-MB-231 cells, but not with cocultures of xCT KD or wildtype SSZ-treated MDA-MB-231 cell inserts (**Fig. 4**), suggesting that peripherally released glutamate may stimulate microglial functional system x_C^- activity.

3.5. MDA-MB-231 carcinoma cells alter microglial protein expression in vitro

The presence of carcinoma cell complete media altered expression of xCT, IRF8, STAT3, and ERK1/2 protein levels in HMC3 microglia (**Fig. 5**). In particular, supplementation with wildtype MDA-MB-231 media increased microglial IRF8, a transcription factor involved in transforming microglia to a reactive state and implicated in microglia-mediated nociception.²⁸ This effect was attenuated in xCT KD cocultures. Lipopolysaccharide increased microglial xCT protein relative to naive HMC3 cells; microglia cocultured with wildtype MDA-MB-231 cells appeared to present marginally more xCT protein than naive cells, although the effect was insignificant. Similarly, MAPK pathway-related proteins (total/phosphorylated STAT3 and total/phosphorylated ERK1/2) were also marginally affected by LPS and cocultures, suggesting that MAPK signalling may be involved in xCT regulation in activated microglia, although these phenomena were slight and insignificant in the present conditions.

4. Discussion

These studies build on the growing body of literature that implicates microglia in the pain state associated with peripheral tumours. To the best of our knowledge, this is the first study to explore the relationship between tumour-released glutamate and microglial xCT with respect to CIP. Our recent work demonstrated that systemic delivery of the microglial inhibitor Pexidartinib delayed the onset and severity of spontaneous tumour-induced nociceptive behaviours and prevented behavioural decline of mechanical withdrawal threshold,³² and several models have previously demonstrated the role of microglia in CIP.^{17,18,23,27,62,65} Our laboratory has also characterized the importance of system x_C^- -released glutamate from tumour cells across various models of CIP.^{32,45,60}

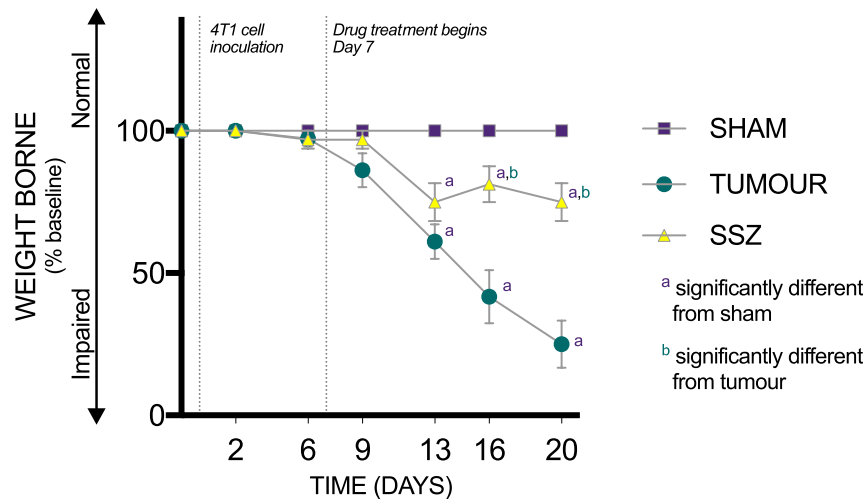


Figure 1. Blockade of system x_C^- with SSZ attenuates CIP. Nociceptive behaviours were quantitated using the DWB in an effort to confirm the translation of our previously validated murine model of CIP to 4T1 tumour cells. 4T1 tumour-bearing mice demonstrated significantly greater nociceptive behaviours relative to sham controls from day 13 after tumour cell inoculation until endpoint, as measured by weight borne in the DWB. This is consistent with previously published data from this model²⁸ and a similar model of CIP from our laboratory using wildtype MDA-MB-231 carcinoma cells in immunocompetent mice.⁵¹ In accordance with data from immunocompromised MDA-MB-231 tumour-bearing mice, treatment with the system x_C^- inhibitor SSZ delayed behavioural decline in 4T1 tumour-bearing mice, as indicated by significantly greater weight borne relative to vehicle-treated mice from day 13 through endpoint. ($P < 0.05$) significantly different from sham (a) and tumour-bearing mice (b), as determined by ANOVA with Bonferroni multiple comparisons. ANOVA, analysis of variance; CIP, cancer-induced pain; DWB, Dynamic Weight Bearing.

Electrophysiological work from murine models of CIP in our laboratory demonstrates sensitization of ascending L4 dorsal root ganglia (DRG) neurons,^{66–68} afferents which release glutamate onto postsynaptic neurons in the dorsal horn upon activation.⁷ Furthermore, we have determined that glutamate directly injected into the hindlimb increases excitability in DRG neurons, an effect that was attenuated by the xCT inhibitor SSZ (unpublished data). Thus, the presence of tumour-derived glutamate initiates physiological changes, which include subsequent glutamate release from DRG neurons, and may contribute to CIP through spinal microglial activation.

Research from this study illustrates the dynamic role of glutamate in microglia-mediated CIP. We have shown that systemically inhibiting system x_C^- activity with SSZ reduces tumour-induced nociceptive behaviours and microglial activation in the dorsal horn. Furthermore, we have demonstrated that extracellular glutamate directly stimulates human HMC3 microglia into their activated state and increases functional system x_C^- activity and expression of xCT, the active antiporter subunit. This activation and functional activity were present in both glutamate-supplemented microglia and those cocultured with glutamate-releasing wildtype, but not xCT knockdown carcinoma cells.

Macrophages release neurotoxic levels of glutamate upon activation by LPS, a potent inflammatory stimulus.^{13,39,40} This effect has been simulated in vivo, in which neurotoxic concentrations of glutamate were released by selectively activated microglia through system x_C^- .²¹ In this study, immunofluorescent costaining of Iba1 and xCT confirmed the ability of LPS to activate HMC3 human microglia in vitro and demonstrated the parallel state of activation in microglia supplemented with complete media from wildtype, but not xCT KD carcinoma cells, further implicating glutamate in microglial activation. In addition, activated microglia presented increased xCT protein levels, while microglia supplemented with xCT KD media presented low xCT protein levels, more comparable with naive microglia than to their wildtype-supplemented counterparts.

Coculture studies demonstrated that wildtype and vector-only MDA-MB-231 carcinoma cells increased microglial functional system x_C^- activity, and this effect was attenuated by xCT knockdown, suggesting that glutamate released by carcinoma cells may be responsible for microglial activation and oxidative burst. Accordingly, the coculture of wildtype, but not xCT knockdown cells, increased microglial protein expression of xCT and IRF8, and slightly increased levels of proteins involved in RAS-MAPK signalling. IRF8, a critical regulator of reactivity in these immune cells, has been previously implicated in microglia-mediated nociception; IRF8-deficient mice are resistant to peripheral nerve injury-induced neuropathic pain, while transferring IRF8-overexpressing microglia spinally to normal mice results in increased nociceptive behaviours.²⁸ Here, protein levels of IRF8 were dramatically increased in microglial cultures treated with LPS and in those cocultured with wildtype MDA-MB-231 cells, an effect which was attenuated in xCT KD cocultures, further supporting the hypothesis that peripherally derived glutamate is involved in the activation of microglia.

STAT3 is also associated with microglial polarization and activation, and macrophage-associated STAT3 has been implicated in tumour progression (reviewed in Ref. 48). MAPK phosphorylates STAT3, which regulates expression of genes, including xCT.²² In MDA-MB-231 breast cancer cells, the MAPK inhibitor PD098059 has been shown to abolish basal xCT transcriptional activity.²² Furthermore, sustained treatment with the STAT3 inhibitor SH-4-54 decreases xCT expression and system x_C^- activity.²²

Behavioural data from 4T1 tumour-bearing mice demonstrated progressive nociception, with significant differences between sham and tumour-bearing mice from day 13 through endpoint. As previously shown by our immunocompromised CIP model,⁶⁰ treatment with SSZ delayed behavioural decline in tumour-bearing mice. In accordance with this and other reports,^{14,49,60} data from this study confirmed the ability of SSZ

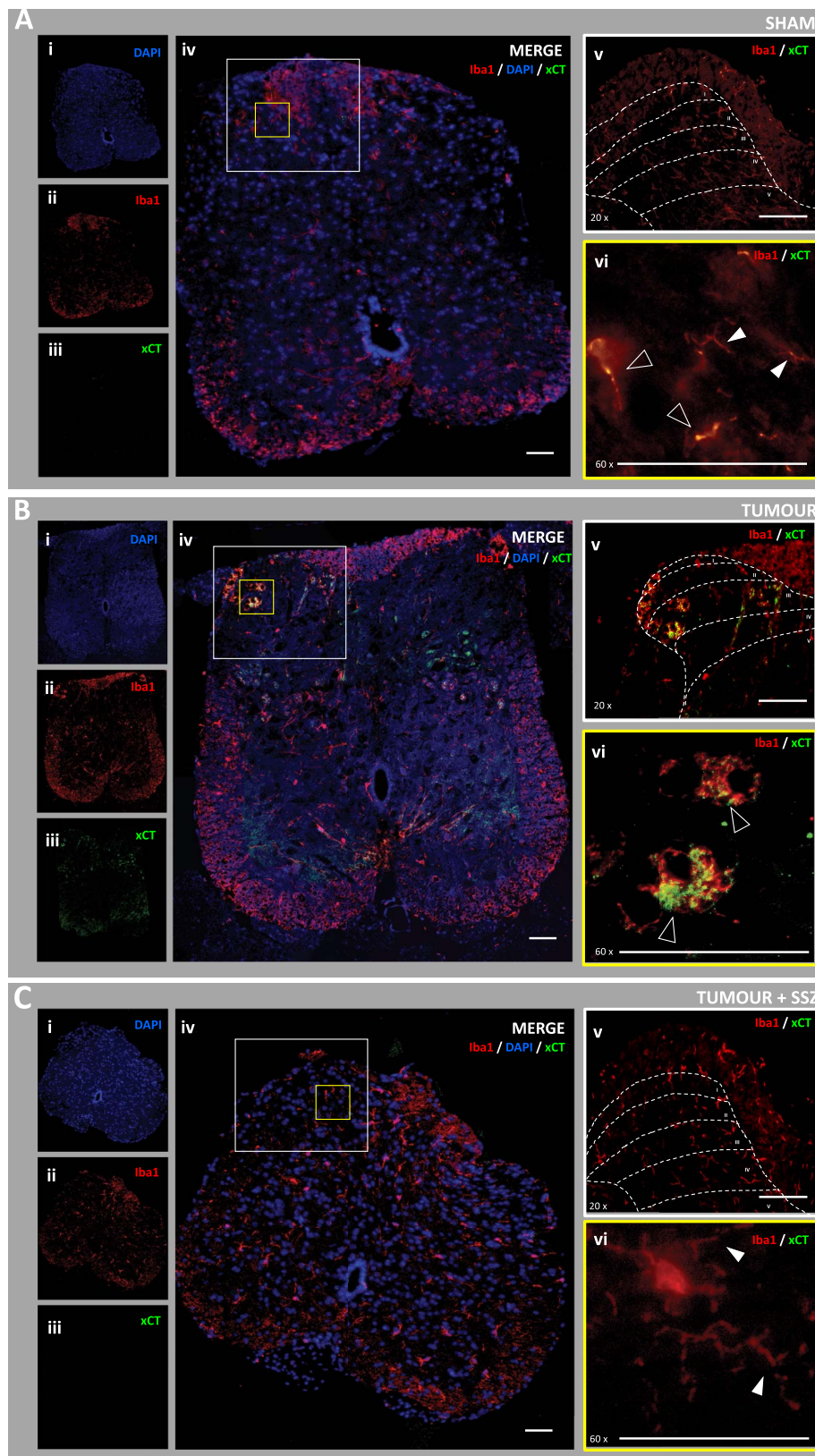


Figure 2. Activated spinal microglial xCT increases in the L4 dorsal horn in tumour-bearing mice. Immunofluorescent staining of nuclei (blue, i), Iba1 (red, ii), and xCT (green, iii), depicting activated microglia and the functional system x_C^- subunit SLC7A11, respectively, in the lumbar 4 dorsal horn of sham (A), tumour + vehicle (B), and tumour + sulfasalazine (SSZ; C) animals. Captures were collected at endpoint (day 20 after tumour inoculation) at 10, 20, and 60 \times magnification and overlaid for double-label Iba1/xCT immunofluorescence (iv). White box indicates 20 \times insert (v), with (i–v) indicating laminae; yellow box indicates 60 \times insert (vi); white arrowheads indicate characteristically ramified microglia, highly branched in morphology; black arrowheads indicate occasions of costaining of Iba1 and xCT. Scale bars = 400 nm.

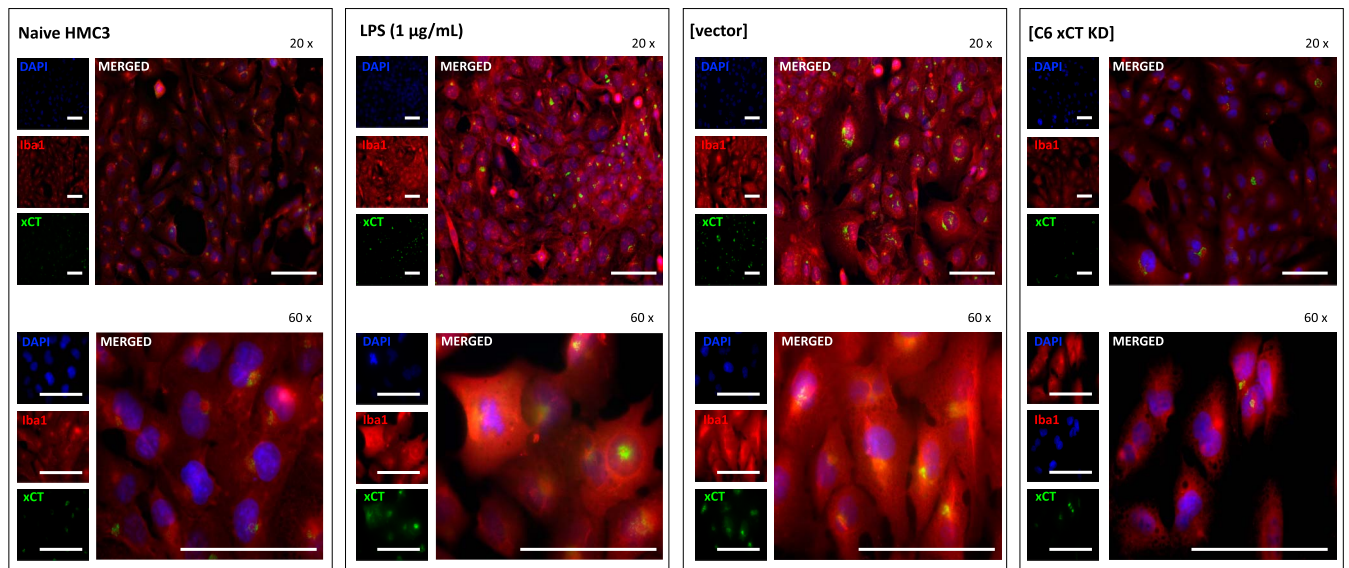


Figure 3. Immunocytochemical costaining of xCT and Iba1 in activated microglia. HMC3 human microglia are activated in the presence of complete media from wildtype, but not xCT knockdown carcinoma cell complete media. Activated microglia demonstrate increased xCT expression, which is attenuated in microglia supplemented with xCT knockdown cell complete media. Chamber slides were stained for nuclei (blue), Iba1 (red), and xCT (green) and imaged using EVOS FL Cell Imaging System at 20× dry (top panel) and 60× oil immersion (bottom panel) lenses. Scale bar = 50 µm. LPS, lipopolysaccharide.

to reduce nociception in an immunocompetent 4T1 carcinoma-induced model of CIP.

Tumour-bearing mice that demonstrated nociception at endpoint also presented robust microglial activation in laminae

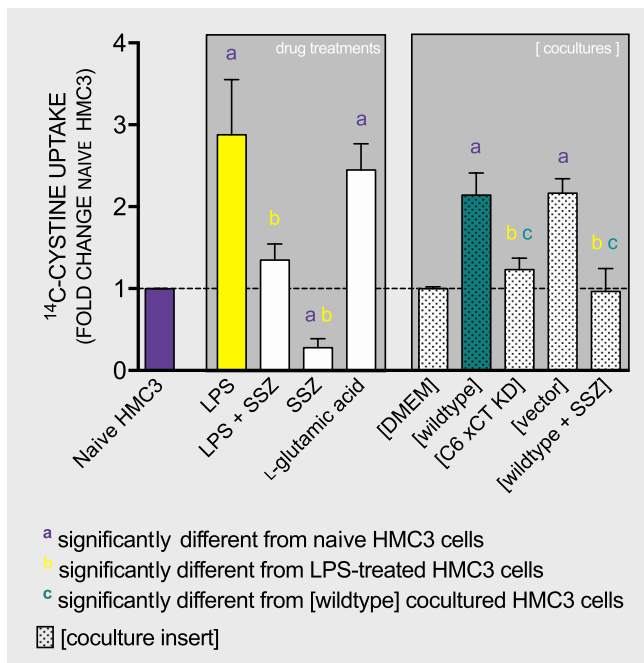


Figure 4. Peripherally released glutamate increases microglial functional system x_C^- activity. SSZ sterically inhibits constitutive and LPS-induced microglial ¹⁴C-cystine uptake in HMC3 human microglia. Treatment with L-glutamic acid increases microglial ¹⁴C-cystine uptake comparable with LPS; coculture with wildtype and vector-only control MDA-MB-231 cells, but not with xCT knockdown cells, increases ¹⁴C-cystine uptake in microglia. Inhibiting MDA-MB-231 cell cocultures with the system x_C^- inhibitor SSZ decreases microglial cystine uptake. ($P < 0.05$) significantly different from naive (a), LPS-treated (b), and wildtype MDA-MB-231 cocultured (c) microglia, as determined by respective *t* tests. LPS, lipopolysaccharide.

I-III of the L4 dorsal horn with vivid costaining of xCT. Conversely, L4 dorsal horn microglia in SSZ-treated tumour-bearing mice were characteristically ramified, with low constitutive staining of Iba1 and negligible levels of xCT^+ costaining. This region of the spinal cord is one in which several microglia-associated factors, including IL-6, IL-1 β , phosphorylated 38 MAPK (p38 MAPK), brain-derived neurotrophic factor, and toll-like receptor 4 (TLR4), have been previously implicated in CIP, with particular prominence in terminals of laminae I-III.²⁹ Thus, upregulated xCT in chronically activated spinal microglia may be one pathway to central microglial-induced glutamate cytotoxicity. SSZ or other system x_C^- targeting agents may therefore represent a potential therapeutic for mitigating chronic spinal microglial activation associated with CIP.

A rapidly growing body of evidence depicts a clear sex difference in immune-mediated pain hypersensitivity, such that female mice are often unaffected by microglia-targeting agents which are effective in their male counterparts (reviewed in Ref. 51). The highly heterogeneous state of bone cancer pain is believed to be the consequence of several pathological mechanisms due to the unique properties of the affected tissue, including vascularization and rich periosteal neuronal networks, immune cells, osteoclasts, and osteoblasts. Bone tumour-induced pathologies have been implicated in the sensitization of surrounding nociceptors, including immune-mediated inflammation,^{2,6} osteoclastogenesis,²⁵ neurogenesis,^{26,46} demyelination,¹⁹ and extracellular acidification.² These pathologies may cumulatively contribute to disparity between cancer-induced hyperalgesia and other chronic pain models. Indeed, several studies have demonstrated promising effects of microglial inhibition across models of CIP in both male and female mice.^{17,18,23,27,50,62,65} Minocycline, a commonly used inhibitor of microglial activation, has been shown to inhibit nociceptive behaviours in murine models of mammary carcinoma cell-induced CIP in male and female mice,^{8,24,50} suggesting the sexual dimorphism commonly observed across several models of chronic pain may not be relevant to CIP.

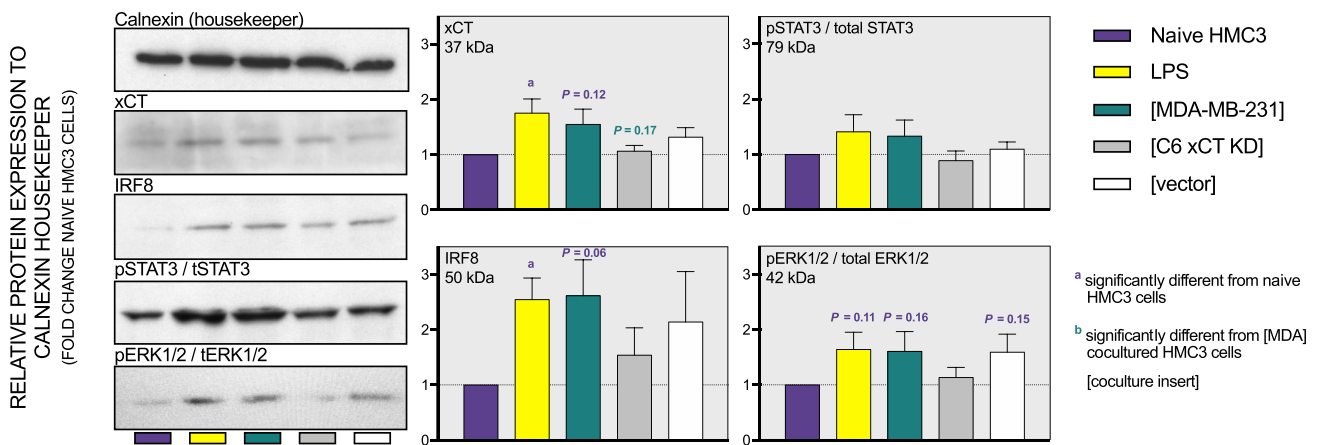


Figure 5. Lipopolysaccharide (LPS) alters microglial protein levels. Western blotting demonstrated the significant increase of microglial IRF8 protein levels in human HMC3 cells stimulated with LPS, with marginal shifts in xCT, pSTAT3, and ERK1/2 protein levels in LPS-stimulated and carcinoma cell cocultured microglia. Bars represent the mean of 3 replicates as a fold change relative to naive HMC3 cells, with error bars indicating SEM; ($P < 0.05$), as determined by planned pairwise comparisons.

Neurons of the CNS have limited capacity for cystine uptake and are reliant primarily on glia for the provision of cysteine for neuronal glutathione production.¹⁵ Relative to neurons, microglia express high levels of the system x_C^- transporter because of a marked need for oxidative protection and are therefore a key source of excitotoxic glutamate. Activated microglia release glutamate through system x_C^- ,³⁸ and most of the glutamate exported from activated microglia can be attributed to the system x_C^- exchange mechanism.^{4,38} This mechanism becomes extremely active in microglia because it is the primary route of internalizing cystine for the production of glutathione. As microglia produce abundant reactive oxygen species, they place themselves under severe oxidative stress. Thus, the microglial oxidative burst creates a glutathione shortage that is alleviated by cystine influx through xCT, extruding glutamate in the balance.⁵

In the presence of high extracellular cystine, microglia become neurotoxic effector cells. This toxicity is selective for neurons and dependent on activation of neuronal ionotropic GluRs. The substances released by activated microglia further activate additional nearby astrocytes, microglia, and neurons, creating a positive feedback loop (reviewed in Ref. 33). Thus, once the harmful stimulus has been managed, it is critical that the microglial inflammatory response be dampened. Immunomodulatory mediators inhibit the release of proinflammatory factors, thereby facilitating a return to homeostasis. In a state of chronic microglial activation, such as that seen in cancer, tumour cells constantly secrete toxic levels of glutamate and disrupt the return to homeostasis. Given the presence of system x_C^- on microglia, nonvesicular glutamate through this antiporter on microglia represents a notable mechanism for glial-neuronal communication.

Data from this study collectively demonstrate that the system x_C^- antiporter is functionally implicated in CIP and may be particularly relevant to pain progression through microglia. Given the increased spinal microglial activation in the tumour-bearing state, the upregulated presence of xCT on microglia in the presence of glutamate-releasing tumour cells, and the implications of system x_C^- in the pain state associated with metastatic tumours, this pathway may be a valuable target for mitigating CIP.

Disclosures

The authors have no conflict of interest to declare.

Acknowledgements

This work was supported by the Canadian Breast Cancer Foundation to G. Singh.

Article history:

Received 12 October 2018

Received in revised form 26 February 2019

Accepted 27 February 2019

References

- Abbadie C, LINDIA JA, Cumiskey AM, Peterson LB, Mudgett JS, Bayne EK, DeMartino JA, MacIntyre DE, Forrest MJ. Impaired neuropathic pain responses in mice lacking the chemokine receptor CCR2. *Proc Natl Acad Sci U S A* 2003;100:7947–52.
- Asai H, Ozaki N, Shinoda M, Nagamine K, Tohnai I, Ueda M, Sugiura Y. Heat and mechanical hyperalgesia in mice model of cancer pain. *PAIN* 2005;117:19–29.
- Bannai S. Exchange of cystine and glutamate across plasma membrane of human fibroblasts. *J Biol Chem* 1986;261:2256–63.
- Barger SW, Basile AS. Activation of microglia by secreted amyloid precursor protein evokes release of glutamate by cystine exchange and attenuates synaptic function. *J Neurochem* 2001;76:846–54.
- Barger SW, Goodwin ME, Porter MM, Beggs ML. Glutamate release from activated microglia requires the oxidative burst and lipid peroxidation. *J Neurochem* 2007;101:1205–13.
- Breese NM, George AC, Pauers LE, Stucky CL. Peripheral inflammation selectively increases TRPV1 function in IB4-positive sensory neurons from adult mouse. *PAIN* 2005;115:37–49.
- Broman J, Anderson S, Ottersen OP. Enrichment of glutamate-like immunoreactivity in primary afferent terminals throughout the spinal cord dorsal horn. *Eur J Neurosci* 1993;5:1050–61.
- Bu H, Shu B, Gao F, Liu C, Guan X, Ke C, Cao F, Hinton AO, Xiang H, Yang H, Tian X, Tian Y. Spinal IFN- γ -induced protein-10 (CXCL10) mediates metastatic breast cancer-induced bone pain by activation of microglia in rat models. *Breast Cancer Res Treat* 2014;143:255–63.
- Cao H, Zhang YQ. Spinal glial activation contributes to pathological pain states. *Neurosci Biobehav Rev* 2008;32:972–83.
- Chen NF, Huang SY, Chen WF, Chen CH, Lu CH, Chen CL, Yang SN, Wang HM, Wen ZH. TGF- β 1 attenuates spinal neuroinflammation and the excitatory amino acid system in rats with neuropathic pain. *J Pain* 2013;14:1671–85.
- Choi DW. Glutamate neurotoxicity and diseases of the nervous system. *Neuron* 1988;1:623–34.
- De Ciantis K, Henry J, Yashpal G, Singh G. Characterization of a rat model of metastatic prostate cancer bone pain. *J Pain Res* 2010;3:213.
- Domercq M, Sánchez-Gómez MV, Sherwin C, Etxebarria E, Fern R, Matute C. System x_C^- and glutamate transporter inhibition mediates microglial toxicity to oligodendrocytes. *J Immunol* 2007;178:6549–56.
- Doxsee DW, Gout PW, Kurita T, Lo M, Buckley AR, Wang Y, Xue H, Karp CM, Cutz JC, Cunha GR, Wang YZ. Sulfasalazine-induced cystine

- starvation: potential use for prostate cancer therapy. *Prostate* 2007;67:162–71.
- [15] Dringen R, Pfeiffer B, Hamprecht B. Synthesis of the antioxidant glutathione in neurons: supply by astrocytes of CysGly as precursor for neuronal glutathione. *J Neurosci* 1999;19:562–9.
- [16] Hendrickx DAE, van Eden CG, Schuurman KG, Hamann J, Huitinga I. Staining of HLA-DR, Iba1 and CD68 in human microglia reveals partially overlapping expression depending on cellular morphology and pathology. *J Neuroimmunol* 2017;309:12–22.
- [17] Hu XF, He XT, Zhou KX, Zhang C, Zhao WJ, Zhang T, Li JL, Deng JP, Dong YL. The analgesic effects of triptolide in the bone cancer pain rats via inhibiting the upregulation of HDACs in spinal glial cells. *J Neuroinflammation* 2017;14:213.
- [18] Huo W, Zhang Y, Liu Y, Lei Y, Sun R, Zhang W, Huang Y, Mao Y, Wang C, Ma Z, Gu X. Dehydrocorydaline attenuates bone cancer pain by shifting microglial M1/M2 polarization toward the M2 phenotype. *Mol Pain* 2018;14:1744806918781733.
- [19] Inoue M, Rashid MH, Fujita R, Contos JJA, Chun J, Ueda H. Initiation of neuropathic pain requires lysophosphatidic acid receptor signaling. *Nat Med* 2004;10:712–8.
- [20] Ji RR, Berta T, Nedergaard M. Glia and pain: is chronic pain a gliopathy? *PAIN* 2013;154:S10–28.
- [21] Kigerl KA, Ankeny DP, Garg SK, Wei P, Guan Z, Lai W, McTigue DM, Banerjee R, Popovich PG. System xc⁻ regulates microglia and macrophage glutamate excitotoxicity in vivo. *Exp Neurol* 2012;233:333–41.
- [22] Linher-Melville K, Haftchenary S, Gunning P, Singh G. Signal transducer and activator of transcription 3 and 5 regulate system Xc⁻ and redox balance in human breast cancer cells. *Mol Cell Biochem*. 2015;405:205–21.
- [23] Liu M, Yao M, Wang H, Xu L, Zheng Y, Huang B, Ni H, Xu S, Zhou X, Lian Q. P2Y₁₂ receptor-mediated activation of spinal microglia and p38MAPK pathway contribute to cancer-induced bone pain. *J Pain Res* 2017;10:417–26.
- [24] Liu X, Bu H, Liu C, Gao F, Yang H, Tian X, Xu A, Chen Z, Cao F, Tian Y. Inhibition of glial activation in rostral ventromedial medulla attenuates mechanical allodynia in a rat model of cancer-induced bone pain. *J Huazhong Univ Sci Technol Med Sci* 2012;32:291–8.
- [25] Lozano-Ondoua AN, Symons-Liguori AM, Vanderah TW. Cancer-induced bone pain: mechanisms and models. *Neurosci Lett* 2013;557:52–9.
- [26] Mantyh WG, Jimenez-Andrade JM, Stake JI, Bloom AP, Kaczmarek MJ, Taylor RN, Freeman KT, Ghilardi JR, Kuskowski MA, Mantyh PW. Blockade of nerve sprouting and neuroma formation markedly attenuates the development of late stage cancer pain. *Neuroscience* 2010;171:588–98.
- [27] Mao-Ying QL, Wang XW, Yang CJ, Li X, Mi WL, Wu GC, Wang YQ. Robust spinal neuroinflammation mediates mechanical allodynia in Walker 256 induced bone cancer rats. *Mol Brain* 2012;5:16.
- [28] Masuda T, Tsuda M, Yoshinaga R, Tozaki-Saitoh H, Ozato K, Tamura T, Inoue K. IRF8 is a critical transcription factor for transforming microglia into a reactive phenotype. *Cell Rep* 2012;1:334–40.
- [29] Meng X, Gao J, Zuo JL, Wang LN, Liu S, Jin XH, Yao M, Namaka M. Toll-like receptor-4/p38 MAPK signaling in the dorsal horn contributes to P2X4 receptor activation and BDNF over-secretion in cancer induced bone pain. *Neurosci Res* 2017;125:37–45.
- [30] Miladinovic T, Nashed MG, Singh G. Overview of glutamatergic dysregulation in central pathologies. *Biomolecules* 2015;5:3112–41.
- [31] Miladinovic T, Sharma M, Phan A, Geres H, Ungard RG, Linher-Melville K, Singh G. Activation of hippocampal microglia in a murine model of cancer-induced pain. *J Pain Res* 2019;12:1003–16.
- [32] Miladinovic T, Ungard RG, Linher-Melville K, Popovic S, Singh G. Functional effects of TrkA inhibition on system xC⁻-mediated glutamate release and cancer-induced bone pain. *Mol Pain* 2018;14:1–15.
- [33] Milligan ED, Watkins LR. Pathological and protective roles of glia in chronic pain. *Nat Rev Neurosci* 2009;10:23–36.
- [34] Murugan M, Ling EA, Kaur C. Glutamate receptors in microglia. *CNS Neurol Disord Drug Targets* 2013;12:773–84.
- [35] Myers RR, Heckman HM, Rodriguez M. Reduced hyperalgesia in nerve-injured WLD mice: relationship to nerve fiber phagocytosis, axonal degeneration, and regeneration in normal mice. *Exp Neurol* 1996;141:94–101.
- [36] Niederberger E, Schmidtko A, Coste O, Marian C, Ehnert C, Geisslinger G. The glutamate transporter GLAST is involved in spinal nociceptive processing. *Biochem Biophys Res Commun* 2006;346:393–9.
- [37] Niederberger E, Schmidtko A, Rothstein JD, Geisslinger G, Tegeder I. Modulation of spinal nociceptive processing through the glutamate transporter GLT-1. *Neuroscience* 2003;116:81–7.
- [38] Piani D, Fontana A. Involvement of the cystine transport system xc⁻ in the macrophage-induced glutamate-dependent cytotoxicity to neurons. *J Immunol* 1994;152:3578–85.
- [39] Piani D, Frei K, Do KQ, Cuénod M, Fontana A. Murine brain macrophages induced NMDA receptor mediated neurotoxicity in vitro by secreting glutamate. *Neurosci Lett* 1991;133:159–62.
- [40] Piani D, Spranger M, Frei K, Schaffner A, Fontana A. Macrophage-induced cytotoxicity of N-methyl-D-aspartate receptor positive neurons involves excitatory amino acids rather than reactive oxygen intermediates and cytokines. *Eur J Immunol* 1992;22:2429–36.
- [41] Pocock JM, Kettenmann H. Neurotransmitter receptors on microglia. *Trends Neurosci* 2007;30:527–35.
- [42] Pulaski BA, Ostrand-Rosenberg S. Mouse 4T1 breast tumor model. Current protocols in immunology. Hoboken: John Wiley & Sons, Inc., 2001, Chapter 20; Unit 20.2.
- [43] Raghavendra V, Tanga F, DeLeo JA. Inhibition of microglial activation attenuates the development but not existing hypersensitivity in a rat model of neuropathy. *J Pharmacol Exp Ther* 2003;306:624–30.
- [44] Sato H, Tamba M, Okuno S, Sato K, Keino-Masu K, Masu M, Bannai S. Distribution of cystine/glutamate exchange transporter, system x(c)⁻, in the mouse brain. *J Neurosci* 2002;22:8028–33.
- [45] Seidlitz EP, Sharma MK, Saikali Z, Ghert M, Singh G. Cancer cell lines release glutamate into the extracellular environment. *Clin Exp Metastasis* 2009;26:781–7.
- [46] Sevcik MA, Ghilardi JR, Peters CM, Lindsay TH, Halvorson KG, Jonas BM, Kubota K, Kuskowski MA, Boustany L, Shelton DL, Mantyh PW. Anti-NGF therapy profoundly reduces bone cancer pain and the accompanying increase in markers of peripheral and central sensitization. *PAIN* 2005;115:128–41.
- [47] Shan S, Qi-Liang MY, Hong C, Tingting L, Mei H, Haili P, Yan-Qing W, Zhi-Qi Z, Yu-Qiu Z. Is functional state of spinal microglia involved in the anti-allodynic and anti-hyperalgesic effects of electroacupuncture in rat model of monoarthritis? *Neurobiol Dis* 2007;26:558–68.
- [48] Sica A, Bronte V. Altered macrophage differentiation and immune dysfunction in tumor development. *J Clin Invest* 2007;117:1155–66.
- [49] Slosky LM, BassiriRad NM, Symons AM, Thompson M, Doyle T, Forte BL, Staatz WD, Bui L, Neumann WL, Mantyh PW, Salvemini D, Largent-Milnes TM, Vanderah TW. The cystine/glutamate antiporter system xc⁻ drives breast tumor cell glutamate release and cancer-induced bone pain. *PAIN* 2016;157:2605–16.
- [50] Song ZP, Xiong BR, Guan XH, Cao F, Manyande A, Zhou YQ, Zheng H, Tian YK. Minocycline attenuates bone cancer pain in rats by inhibiting NF-κB in spinal astrocytes. *Acta Pharmacol Sin* 2016;37:753–62.
- [51] Sorge RE, Mapplebeck JCS, Rosen S, Beggs S, Taves S, Alexander JK, Martin LJ, Austin JS, Sotocinal SG, Chen D, Yang M, Shi XQ, Huang H, Pillion NJ, Bilan PJ, Tu Y, Klip A, Ji RR, Zhang J, Salter MW, Mogil JS. Different immune cells mediate mechanical pain hypersensitivity in male and female mice. *Nat Neurosci* 2015;18:1081–3.
- [52] Streit WJ. Microglia as neuroprotective, immunocompetent cells of the CNS. *Glia* 2002;40:133–9.
- [53] Sun S, Cao H, Han M, Li TT, Zhao ZQ, Zhang YQ. Evidence for suppression of electroacupuncture on spinal glial activation and behavioral hypersensitivity in a rat model of monoarthritis. *Brain Res Bull* 2008;75:83–93.
- [54] Sweitzer SM, Schubert P, DeLeo JA. Propentofylline, a glial modulating agent, exhibits antiallostatic properties in a rat model of neuropathic pain. *J Pharmacol Exp Ther* 2001;297:1210–7.
- [55] Tahrarou SL, Marret S, Bodénan C, Leroux P, Dommergues MA, Evrard P, Gressens P. Central role of microglia in neonatal excitotoxic lesions of the murine periventricular white matter. *Brain Pathol* 2001;11:56–71.
- [56] Tofaris GK, Patterson PH, Jessen KR, Mirsky R. Denervated Schwann cells attract macrophages by secretion of leukemia inhibitory factor (LIF) and monocyte chemoattractant protein-1 in a process regulated by interleukin-6 and LIF. *J Neurosci* 2002;22:6696–703.
- [57] Tsuda M. Microglia in the spinal cord and neuropathic pain. *J Diabetes Investig* 2016;7:17–26.
- [58] Tsuda M, Inoue K, Salter MW. Neuropathic pain and spinal microglia: a big problem from molecules in “small” glia. *Trends Neurosci* 2005;28:101–7.
- [59] Ungard RG, Linher-Melville K, Nashed M, Sharma M, Wen J, Singh G. xCT knockdown in human breast cancer cells delays onset of cancer-induced bone pain. *Mol Pain* 2019;15:1–14.

- [60] Ungard RG, Seidlitz EP, Singh G. Inhibition of breast cancer-cell glutamate release with sulfasalazine limits cancer-induced bone pain. *PAIN* 2014;155:28–36.
- [61] Walter L, Neumann H. Role of microglia in neuronal degeneration and regeneration. *Semin Immunopathol* 2009;31:513–25.
- [62] Wang LN, Yang JP, Zhan Y, Ji FH, Wang XY, Zuo JL, Xu QN. Minocycline-induced reduction of brain-derived neurotrophic factor expression in relation to cancer-induced bone pain in rats. *J Neurosci Res* 2012;90:672–81.
- [63] Watanabe H, Bannai S. Induction of cystine transport activity in mouse peritoneal macrophages. *J Exp Med* 1987;165:628–40.
- [64] Watkins LR, Martin D, Ulrich P, Tracey KJ, Maier SF. Evidence for the involvement of spinal cord glia in subcutaneous formalin induced hyperalgesia in the rat. *PAIN* 1997;71:225–35.
- [65] Yang Y, Li H, Li TT, Luo H, Gu XY, Lü N, Ji RR, Zhang YQ. Delayed activation of spinal microglia contributes to the maintenance of bone cancer pain in female Wistar rats via P2X7 receptor and IL-18. *J Neurosci* 2015;35:7950–63.
- [66] Zhu YF, Kwiecien JM, Dabrowski W, Ungard R, Zhu KL, Huizinga JD, Henry JL, Singh G. Cancer pain and neuropathic pain are associated with A β sensory neuronal plasticity in dorsal root ganglia and abnormal sprouting in lumbar spinal cord. *Mol Pain* 2018;14:1744806918810099.
- [67] Zhu YF, Ungard R, Seidlitz E, Zagal N, Huizinga J, Henry JL, Singh G. Differences in electrophysiological properties of functionally identified nociceptive sensory neurons in an animal model of cancer-induced bone pain. *Mol Pain* 2016;12:174480691662877.
- [68] Zhu YF, Ungard R, Zagal N, Huizinga JD, Henry JL, Singh G. Rat model of cancer-induced bone pain: changes in nonnociceptive sensory neurons in vivo. *Pain Rep* 2017;2:e603.